European Journal of Pharmaceutics and Biopharmaceutics 195 (2024) 114077

Contents lists available at ScienceDirect

European Journal of Pharmaceutics and Biopharmaceutics

journal homepage: www.elsevier.com/locate/ejpb

Research paper

Evaluating how cationic lipid affects mRNA-LNP physical properties and biodistribution

Claire Guéguen, Thibaut Ben Chimol, Margaux Briand, Kassandra Renaud, Mélodie Seiler, Morgane Ziesel, Patrick Erbacher, Malik Hellal *

Polyplus, 75 rue Marguerite Perey, 67400 Illkirch-Graffenstaden, France

ARTICLE INFO

Keywords:
Cationic lipid
mRNA delivery
Lipid nanoparticles (LNPs)
Vaccines
Transfection
In vivo delivery
Imidazolium-based lipid

ABSTRACT

RNA therapeutics represents a powerful strategy for diseases where other approaches have failed, especially given the recent successes of mRNA vaccines against the coronavirus disease 2019 (COVID-19) and small interfering (siRNA) therapeutics. However, further developments are still required to reduce toxicity, improve stability and biodistribution of mRNA-LNPs (lipid nanoparticles). Here, we show a rational combinatorial approach to select the best formulation based on a new cationic lipid molecule **(IM21.7c)**, which includes an imidazolium polar head. The study allowed us to select the optimal 5 lipids composition for *in vivo* mRNA delivery. **IM21.7c** based mRNA-LNPs measuring less than 100 nm had high encapsulation efficiency, protected mRNA from degradation, and exhibited sustained release kinetics for effective *in vitro* transfection. Most interestingly the biodistribution was significantly different from other clinically approved LNPs, with increased targeting to the lung. Further studies are now required to expand the possible applications of these new molecules.

1. Introduction

Research in lipid nanoparticles (LNPs) for nucleic acid delivery has culminated after the approval of the first antisense RNA (RNAi) therapeutics (Onpattro®) approved by both the US FDA and EMA in 2018, and more recently the tremendous success of mRNA vaccines against the coronavirus disease 2019 (COVID-19; Pfizer-BioNTech's Comirnaty® and Moderna's Spikevax®) [1,2,3]. mRNA COVID-19 vaccines rapidly adopted LNPs due to their ease of production, and protective properties. They are also effective for vaccination following intramuscular injection as they act as adjuvants and improve vaccine reactogenicity [4].

These successes heavily rely on the LNP delivery systems, which acts as a protective capsule for the nucleic acid, ensuring effective delivery to the cytosol. Onpattro® is used for the treatment of ATTR (Transthyretin Amyloidosis) and consists in LNPs delivering small interfering RNA (siRNA) to the liver to silence the expression of Transthyretin protein. Many studies are currently also assessing LNP delivery for a range of molecules such as antisense oligonucleotides (ASOs), microRNA, DNA and self-amplifying RNA (saRNA and samRNA) including preclinical and clinical trials developing *in vivo* CRISPR/Cas9 treatments for *in vivo* gene editing [5–7].

With the current shift toward precision medicine, LNPs also represent versatile and tuneable systems for drug delivery [8,9] and more specifically mRNA delivery. It is crucial however that new developments follow a rational design to fulfil all LNPs functions including structure and morphology; encapsulation of nucleic acid or protein uptake as well as endosomal escape; size, low heterogeneity/polydispersity, storage and stability; *in vivo* stability and organ targeting.

LNPs form micellar structures within the particle core and are composed of four main building blocks: (1) cationic lipids, (2) a polyethylene glycol (PEG)-lipid conjugate and helper lipids such as (3) phospholipids and (4) sterols. Each of these lipids promote different features of the LNPs (Fig. 1). Ionizable cationic lipids serve two main functions including facilitating the nucleic acid encapsulation through interaction with negatively charged nucleic acids and mediating endosome disruption to enable nucleic acid release to the cytoplasm; all mediated via a pH-depending quaternary ammonium group. PEG-lipids are usually the smallest molar percentage of the lipid composition of an LNP. They influence population charge, size and dispersity and prevent LNP aggregation while enhancing particle stability and thus playing a key role in circulation and biodistribution. Helper and structural lipids broadly define a range of lipids that are typically non-cationic such as phospholipids and sterols. They mostly support particle structure and enhance stability during storage and circulation. Cholesterol is known to

* Corresponding author.
E-mail address: mhellal@polyplus-transfection.com (M. Hellal).

https://doi.org/10.1016/j.ejpb.2023.08.002
Received 30 May 2023; Received in revised form 2 August 2023; Accepted 7 August 2023
Available online 12 August 2023

reduce the amount of surface bound protein and to improve circulation as well as half-life. Similarly, phospholipids also play a role in encapsulation, particle structure and cellular delivery.

The standard use of 4 lipid components leads to countless LNP formulations, which require a deep understanding of the physicochemical properties of the various LNP building blocks and a knowledge of how LNP morphology is altered based on formulation and structural parameters [10,11]. Historically, cationic liposomes were among the earliest synthetic systems used for this purpose based on cationic lipids (such as DOTAP and DOTMA shown in Fig. 1). Progressively PEGylated lipids were added to formulations and later ionizable lipids replaced widely used DOTAP [12]. New formulations including ionizable lipids such as Dlin-MC3-DMA were shown to form LNPs and increase the mRNA concentration within the LNP (Fig. 1).These clinically approved ionizable lipids are neutral at physiological pH and protonated at low pH, which enhance endosomal escape [13]. Other approaches consisted in replacing helper lipids with charged alternatives with the goal to promote the biodistribution to the lung and the spleen [14]. More recently, the focus shifted to improving the efficiency of mRNA-LNP delivery and their stability. For example, detailed studies describe the effect of LNP size and composition on *in vitro* transfection efficiency [15] and *in vivo* biodistribution [16] while others further elucidate mRNA encapsulation and particle structure [17], paving the way for a new wave of rational design of mRNA-LNP. Even novel surface modifications have been incorporated to modify the surface charge and increase the interaction with mucus found in the epithelia mucosae [18] to improve *in vivo* delivery.

The ionizable cationic lipid within the LNP is considered a key component that determines potency, mRNA delivery efficiency, as well as degradability and reactogenicity. It even displays adjuvant properties. Therefore, many groups have focused on developing new ionizable lipids, for example, the inclusion of imidazole modified lipids or new ionizable lipids improved mRNA stability and delivery [19,20,21,22,23,13] including an understanding of how ionization and structure properties influence expression depending on the administration route [24].

Lipid-based nanoparticles represent one of the most promising RNA delivery systems, not only due to their efficacy, but also to the ease of production achieved through precise controlled mixing technique known as microfluidics [25–28] and the scalability of production. Still, they present limitations related to toxicity [29] and targeting. Furthermore, the biodistribution is restricted through systemic administration, mainly resulting in an uptake in the liver and the spleen; and sometimes in the lung [30,31], limiting possible applications to therapeutic vaccination, oncology or gene-editing. Further developments and improved formulations are therefore needed to solve these main limitations.

In this study we aimed to develop a novel type of mRNA-LNP with a permanent positive charge, like formulations based on cationic lipids, with a low toxicity profile similar to clinically approved LNPs but with a different biodistribution, namely a lung tropism instead of preferential accumulation/uptake by the liver hepatocytes through systemic application. We hypothesised that positively charged circulating mRNA-LNPs with particle sizes below 100 nm, are likely to be trapped in the lung and bind to the anionic endothelial cells surface, increasing cell entry and nucleic acid delivery, similarly to lipoplexes or polyplexes. To validate this hypothesis, we first needed to synthesise a new cationic lipid with reduced toxicity compared to the main reference of permanently charged cationic lipids, DOTMA and DOTAP. To do so, we removed the charge from the quaternary ammonium, and synthetized a new N-heterocycle, imidazolium, that carried the charge. We previously demonstrated the efficiency of this family of molecules to transfect both *in vitro* and *in vivo* mRNA through liposome-based delivery. Based on these results, **IM21.7c** has been selected to investigate the use of imidazolium in mRNA-LNP formulation. A 7-step synthesis has been developed to afford **IM21.7c** in an 37.2 % overall yield (Scheme 1).

Exploiting the properties of **IM21.7c**, our combinatorial approach consisted in the preparation and evaluation a range of lipid compositions and ratios to select the most effective IM21.7c-based LNP for mRNA delivery *in vitro* and *in vivo,* as a proof of concept leading to the demonstration that imidazolium is required to produce safe, effective, and stable LNPs.

2. Materials and methods

2.1. Materials

IM21.7c was obtained from Polyplus. 1,2-dioleoyl-3-trimethylammonium-propane (DOTAP), 2-dioleyloxy-N,N-dimethyl-3-

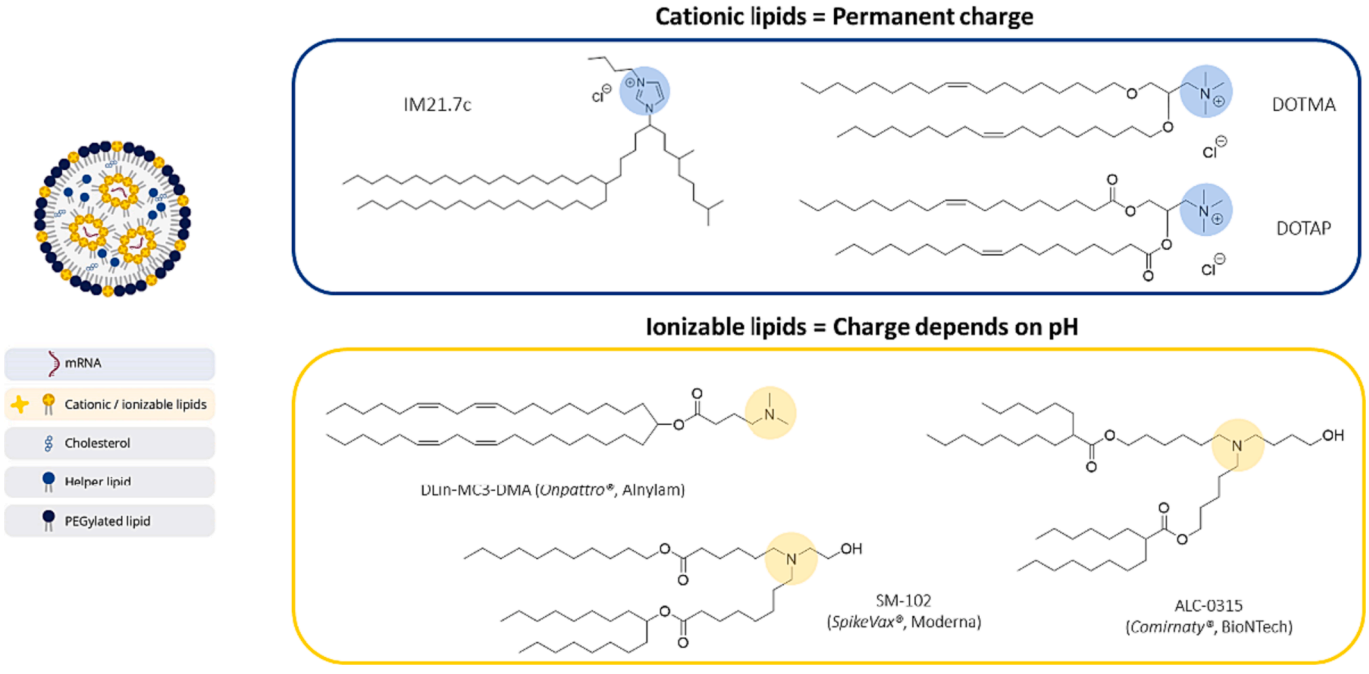

Fig. 1. Schematic representation of mRNA-LNP and structures of cationic and ionizable lipids.

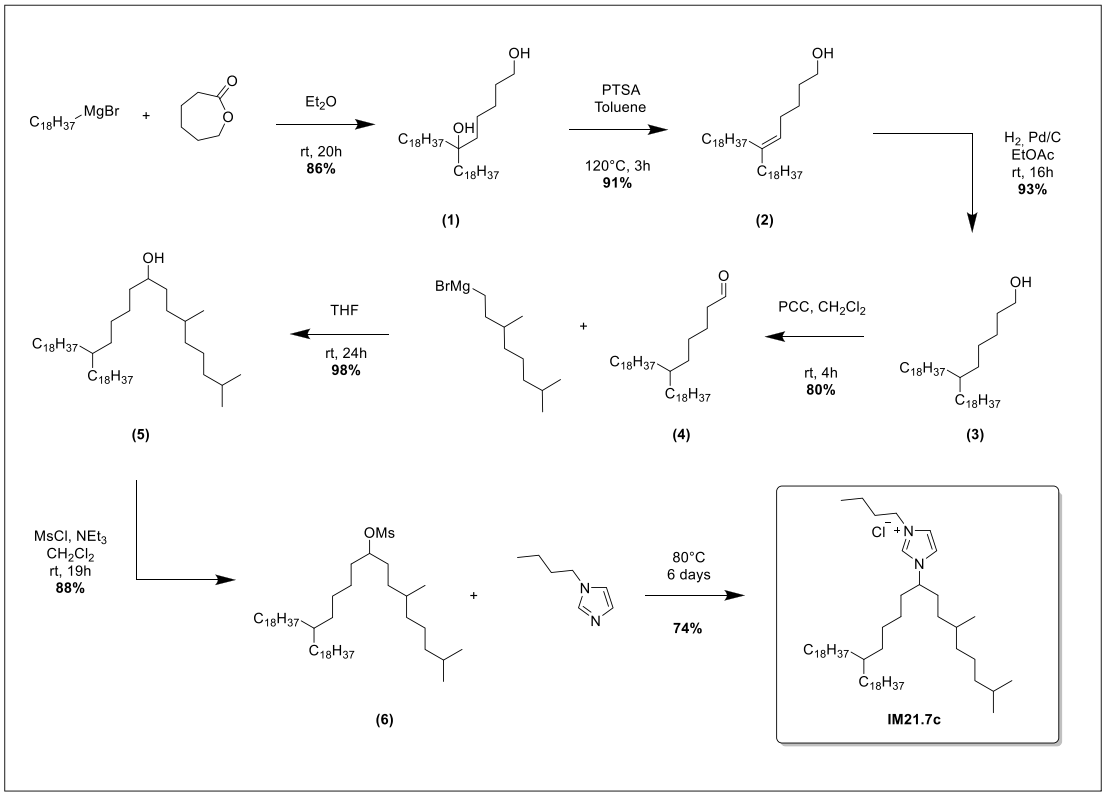

Scheme 1. Synthesis of IM21.7c: 1-butyl-3-(2,6-dimethyl-14-octadecyldotriacontan-9-yl)-1H-imidazol-3-ium chloride.

aminopropane (DODMA), 1,2-di-O-octadecenyl-3-trimethylammonium propane (DOTMA), 1,2-diphenytanoyl-*sn*-glycero-3-phosphoethanolamine (DPyPE) and cholesterol were purchased from Avanti Polar Lipids (Alabaster, AL). (6Z,9Z,28Z,31Z)-heptatriacont-6,9,28,31-tetraene-19-yl 4-(dimethylamino)-butanoate (DLin-MC3-DMA) was purchased from Cayman Chemicals (Ann Arbor, MI). 1,2-Dimyristoyl-*sn*-glycero-3-methoxypolyethylene glycol (DMG-PEG), 1,2-Distearoyl-*rac*-glycero-3-methylpolyoxyethylene (DSG-PEG). Heptadecan-9-yl 8-{(2-hydroxyethyl)[6-oxo-6-(undecyloxy)hexyl]amino}octanoate (SM-102) and [(4-Hydroxybutyl)azanediyl]di(hexane-6,1-diyl) bis(2-hexyldecanoate) (ALC-0315) have been purchased from Avanti Polar Lipids, Inc. CleanCap® Firefly Luciferase (FLuc) mRNA (5-methoxyuridine) was obtained from TriLink BioTechnologies (San Diego, CA). Human Caco-2 epithelial cells from colorectal adenocarcinoma were purchased from American Type Culture Collection (ATCC, Manassas, VA). Fetal Bovine Serum (FBS) was obtained from Biowest. Cells were cultured in DMEM medium (Lonza) supplemented with FBS (20% v:v), non-essential amino acid Solution (1% v:v, Thermo Fisher Scientific), sodium pyruvate (1% v:v, Sigma-Aldrich), L-glutamine (1% v:v, Sigma-Aldrich) and penicillin/streptomycin (2% v:v, Thermo Fisher Scientific) in a humidified incubator with 5% CO_2 at 37 °C.

2.2. Synthesis of ***IM21.7c***

(a) 6-octadecyltetracosane-1,6-diol **(1)**.

To a solution of 100 mL of octadecylmagnesium chloride at 0.5 M in THF (50 mmoles) was added dropwise 2.51 mL of ε-Caprolactone (2.58 g; 22.65 mmoles; MW = 114.14) dissolved in 20 mL diethyl ether. The obtained reaction mixture was stirred under an argon atmosphere at room temperature for 24 h. Then, the reaction mixture was poured onto 600 mL split ice, acidified with concentrated hydrochloric acid for 1 h. The solid residue in suspension was filtered off and washed with water. The solid thus obtained was recrystallized from acetone and dried to afford 12.2 g of pure diol **(1)** (19.58 mmoles; MW = 623.13, 86% yield).

TLC: Rf = 0.25; solvent: ethyl acetate-heptane 3:7 (V:V); detection with vanillin/sulfuric acid (Merck TLC plates silica gel 60 F_{254}).

^{1}H NMR (400 MHz, $CDCl_3$): d = 3.63 (t, *J* = 6.6 Hz, 2H), 1.57 (quint, *J* = 6.7 Hz, 2H), 1.45–1.05 (m, 74H), 0.86 (t, *J* = 6.9 Hz, 6H).

(b) Synthesis of 6-octadecyltetracos-5-en-1-ol **(2)**.

Diol **(1)** (12.2 g; 19.58 mmoles; MW = 623.13) and *p*-toluenesulfonic acid monohydrate (750 mg; 3.9 mmoles; MW = 190.22) were dissolved in 300 mL toluene. The mixture was refluxed for 3 h, water was removed with a Dean-Stark trap. The solvents were removed under reduced pressure to give a crude that was chromatographed on silica gel (CH_2Cl_2-Heptane 1:1) to afford 10.80 g of pure alcenol **(2)** (mixture of isomers) (17.85 mmoles; MW = 605.12, 91% yield).

TLC: Rf = 0.35; solvent: CH_2Cl_2-Heptane 7:3; detection with vanillin/sulfuric acid (Merck TLC plates silica gel 60 F_{254}).

^{1}H NMR (400 MHz, $CDCl_3$): d = 5.11–5.03 (m, 1H), 3.62 (td, *J* = 6.6 Hz, 1.9 Hz, 2H), 2.03–1.89 (m, 6H), 1.60–1.51 (m, 2H), 1.49–0.99 (m, 66H), 0.86 (t, *J* = 6.8 Hz, 6H).

(c) 6-octadecyltetracosan-1-ol **(3)**.

Mixture of alcenol isomers **(2)** (10.80 g, 17.85 mmoles, MW = 605.12) was dissolved in 300 mL ethyl acetate and catalytic hydrogenation with Palladium on charcoal (Pd/C 10%, 2 g) for 24 h at 1 atmosphere pressure of hydrogen was applied. After replacement of hydrogen by argon, the mixture was filtered through Celite® 545. The filter cake was washed with 2 × 250 mL of hot CH_2Cl_2. Combined solvents were removed under reduced pressure to afford 10.10 g of pure alcohol **(3)** (16.63 mmoles, MW = 607.13, 93% yield).

TLC: Rf = 0.35; solvent: CH_2Cl_2-Heptane 7:3; detection with vanillin/sulfuric acid (Merck TLC plates silica gel 60 F_{254}).

^{1}H NMR (400 MHz, $CDCl_3$): d = 3.62 (t, *J* = 6.7 Hz, 2H), 1.55 (quint, *J* = 6.9 Hz, 2H), 1.44–1.00 (m, 75H), 0.86 (t, *J* = 6.7 Hz, 6H).

(d) 6-octadecyltetracosanal **(4)**.

Alcohol **(3)** (10.10 g, 16.63 mmoles, MW = 607.13) was dissolved in 300 mL CH_2Cl_2, Pyridinium chlorochromate (7 g, 32.47 mmoles, MW = 215.56) was added and the reaction stirred at room temperature for 3 h

under an argon atmosphere. The mixture was filtered through Celite® 545 and the filter cake was washed with CH_2Cl_2. Combined solvents were removed under reduced pressure and the obtained crude was chromatographed on silica gel (CH_2Cl_2-Heptane 1:4) to afford 8.08 g of pure aldehyde **(4)** (13.35 mmoles, MW = 605.12, 80% yield).

TLC: Rf = 0.35; solvent: CH_2Cl_2-Heptane 3:7; detection with vanillin/sulfuric acid (Merck TLC plates silica gel 60 F_{254}).

^{1}H NMR (400 MHz, $CDCl_3$): d = 9.74 (t, J = 2.0 Hz, 1H), 2.40 (td, J = 7.3 Hz, 2.0 Hz, 2H), 1.59 (quint, J = 7.3 Hz, 2H), 1.36–1.12 (m, 73H), 0.86 (t, J = 6.9 Hz, 6H).

(e) 2,6-dimethyl-14-octadecyldotriacontan-9-ol **(5)**.

Aldehyde **(4)** (8.08 g, 13.35 mmoles, MW = 605.12) was dissolved in 100 mL THF and then introduced dropwise on 50 mL of a stirred solution of 3,7-Dimethyloctylmagnesium bromide at 1 M in diethyl ether (50 mmoles). The obtained reaction mixture was stirred under an argon atmosphere at room temperature for 24 h. Then, the reaction mixture was poured onto 600 mL split ice, acidified with concentrated chlorhydric acid for 1 h. This solution was then extracted with 3 × 200 mL of CH_2Cl_2, dried over anhydrous sodium sulfate and solvents were removed under reduced pressure. The residue was then resuspended in 200 mL of Acetone and cooled in an ice-water bath for 1 h. Desired product precipitated as a white solid that was recovered by filtration. After drying, 9.80 g of alcohol **(5)** were obtained (13.11 mmoles, MW = 747.40, 98% yield).

TLC: Rf = 0.40; solvent: CH_2Cl_2-Heptane 3:7; detection with vanillin/sulfuric acid (Merck TLC plates silica gel 60 F_{254}).

^{1}H NMR (400 MHz, $CDCl_3$): d = 3.75–3.50 (m, 1H), 1.63–0.96 (m, 89H), 0.92–0.75 (m, 15H).

(f) 2,6-dimethyl-14-octadecyldotriacontan-9-yl methanesulfonate **(6)**.

Alcohol **(5)** (9.80 g; 13.11 mmoles; MW = 747.40) was dissolved in 250 mL of dry CH_2Cl_2 and 18 mL of triethylamine (13.07 g; 129.16 mmoles; MW = 101.19) were added followed by 8 mL of methanesulfonyl chloride (11.84 g; 103.36 mmoles; MW = 114.55) introduced drop-wise. The mixture was stirred overnight at room temperature. After removal of the solvents under reduced pressure, the residue was dissolved in 200 mL of methanol and cooled in an ice-water bath for 1 h. Desired product precipitated as a white solid collected by filtration on a filter paper. After solubilization in CH_2Cl_2 and evaporation, 9.60 g of compound **(6)** were obtained (11.63 mmoles, MW = 825.49, 88% yield).

^{1}H NMR (400 MHz, $CDCl_3$): d = 4.66 (quint, J = 5.9 Hz, 1H), 2.97 (s, 3H), 1.76–1.59 (m, 4H), 1.57–0.98 (m, 85H), 0.91–0.78 (m, 15H).

(g) 1-butyl-3-(2,6-dimethyl-14-octadecyldotriacontan-9-yl)-1H-imidazol-3-ium chloride **IM21.7c**.

Mesylate **(6)** (9.60 g; 11.63 mmoles; MW = 825.49) was resuspended in 40 mL of 1-butylimidazole and was stirred at 80 °C for 5 days under an argon atmosphere. The mixture was diluted with 400 mL of methanol and insoluble matter was removed by filtration. Filtrate was cooled in an ice-water bath, slowly acidified with 100 mL of hydrochloric acid 37% and evaporated to dryness. The residue was resuspended in 400 mL of ultra-pure water and cooled in an ice-water bath for 1 h. Desired product, insoluble in water, was collected by filtration on a filter paper. The obtained residue was further chromatographed on silica gel (CH_2Cl_2-methanol 98:2) to afford 6.78 g of compound **IM21.7c** as a white solid (7.62 mmoles, MW = 890.03, 74% yield).

TLC: Rf = 0.45; solvent: CH_2Cl_2-methanol 9:1; detection with iodine (Merck TLC plates silica gel 60 F_{254}).

^{1}H NMR (400 MHz, $CDCl_3$): d = 11.30 (s, 1H), 7.23–7.20 (m, 1H), 7.13–7.07 (m, 1H), 4.54–4.45 (m, 1H), 4.41 (t, J = 7.3 Hz, 2H), 1.98–1.64 (m, 8H), 1.54–0.98 (m, 88H), 0.88–0.77 (m, 15H).

2.3. mRNA-containing LNP fabrication

All lipids were dissolved in ethanol at a various concentration: IM21.7c, DOTMA, DOTAP, SM-102 and ALC-0315 (100 mM), DODMA and DLin-MC3-DMA (50 mM), DPyPE (30 mM), DSPC or DOPE (50 mM), and cholesterol (50 mM), DMG-PEG and DSG-PEG (10 mM) and final molar ratios established as shown in Table 1. FLuc mRNA was diluted in 10 mM sodium acetate pH 4 buffer prior to LNP fabrication. mRNA containing LNPs were prepared by combining the lipid and mRNA solutions in a NanoAssemblr™ microfluidic cartridge (Precision NanoSystems, Vancouver, BC) at a speed of 10 mL/min and volumetric ratio of 3:1, followed by removal of ethanol with Amicon or Vivaspin centrifugal filter units (10 kDa cutoff). LNPs were filtrated with PES filter 0.45 μm 17 mm and diluted in PBS.

2.4. LNP characterization

Lipid nanoparticles were characterized for size, surface zeta potential, and polydispersity index (PDI) using dynamic light scattering (DLS, Malvern Zetasizer, Worcestershire, UK). Prior to ZetaSizer analysis, the LNPs were diluted twenty-fold in water to a concentration of 2.5 μg/mL mRNA. mRNA concentration in LNPs and encapsulation efficiency of LNPs were determined by modified fluorescent Quant-iT™ RiboGreen™ RNA Assay Kit (ThermoFisher Scientific) according to manufacturer instructions. Briefly, LNPs were diluted in Tris-EDTA buffer or 2% Triton X-100 in Tris-EDTA buffer and incubated at 37 °C for 30 min. Then, RiboGreen reagent was added to each sample and the fluorescence (ex/em 485/520 nm) was read on FLUOstar® Omega microplate reader (BMG Labtech). Encapsulation efficiency (EE) was determined using the following equation:

$$EE(\%) = \frac{totalmRNA - freemRNA}{totalmRNA} x100$$

2.5. mRNA transfection evaluation

LNP-based FLuc mRNA transfection was evaluated in epithelial cells from colorectal adenocarcinoma (Caco-2). 40,000 Caco-2 cells were seeded per well of 24-well plates in complete medium 1 day before transfection. On the day of transfection, 500 ng of LNPs were simply added dropwise to cells in their complete growth medium.

imidazolium-based LNP transfection was evaluated in different cell lines: Caco-2 cells, epithelial cells of cervix adenocarcinoma (HeLa), cells from a liver hepatocellular carcinoma (HepG2) and alveolar epithelial cells (A549). For transfection experiments, 40,000 Caco-2 cells, 50,000 HeLa cells, 100,000 HepG2 cells or 60,000 A549 cells were seeded per well of 24-well plates in complete medium 1 day before transfection. On the day of transfection, 500 ng (Caco-2, HepG2 and A549) or 250 ng (HeLa) of FLuc-encoding mRNA-LNPs were simply added dropwise to cells in their complete growth medium. LNP Comirnaty-like was used as a positive transfection control (ALC-0315 4.63 mM, DSPC 0.94 mM, Chol 4.27 mM and DMG-PEG 0.16 mM).

After 24 h, cells were washed in Phosphate-buffer saline (PBS) × 1 and lysed using cell lysis buffer × 1 (PROMEGA). Luciferase expression was assessed on 2 μL of organ lysate supernatant using 50 μL of luciferin solution (Promega) and sample protein content was evaluated through Pierce BCA Assay Protein Kit (Thermo-fisher). The transfection efficiency (TE) was expressed as relative lights units (RLU) per mg of proteins.

2.6. Animal experiments

All animal studies were conducted in accordance with the French Animal Care guidelines and protocols were approved by the Direction des Services Vétérinaires. Six-week-old female OF1 mice 22–24 g were obtained from Charles River Laboratories (Lyon, France) and subjected to a week of quarantine and acclimation period before use.

Table 1
Details of mRNA-LNP formulation for *in vitro* evaluation.

LNP N°	Cationic lipid (mM)		Ionizable lipid (mM)		Helper lipid (mM)		Cholesterol (mM)	DSG-PEG_{2k} (mM)	Size (d.nm)	PDI	Zeta (mV)	EE (%)
1	IM21.7c	4	DODMA	3	DPyPE	1	1.85	0.15	64 ± 2	0.068	+12	98%
2	IM21.7c	0	DODMA	3	DPyPE	1	1.85	0.15	32 ± 3	0.156	0	93%
3	IM21.7c	4	DODMA	0	DPyPE	1	1.85	0,15	71 ± 3	0.152	+17	98%
4	IM21.7c	4	DLin-MC3-DMA	3	DPyPE	1	1.85	0.15	80 ± 3	0.077	+12	ND
5	IM21.7c	2	DODMA	5	DPyPE	1	1.85	0.15	51 ± 1	0.131	+11	99%
6	IM21.7c	3	DODMA	3	DPyPE	1	2.85	0.15	43 ± 1	0.085	+9	98%
7	IM21.7c	4	DODMA	2	DPyPE	1	1.85	0.15	61 ± 3	0.11	+12	97%
8	DOTAP	4	DODMA	3	DPyPE	1	1.85	0.15	40 ± 1	0.018	+12	86%
9	DOTMA	4	DODMA	3	DPyPE	1	1.85	0.15	35 ± 2	0.1788	+12	95%
10	IM21.7c	4	DODMA	3	DPyPE	1	1.70	0.3	32 ± 1	0.221	+17	99%
11	IM21.7c	4	DODMA	3	DPyPE	1	1.50	0.5	22 ± 2	0.292	+12	98%

ND: non-determined.
Lipid composition (molar concentration), size (nm), polydispersity index (PDI), zeta potential (mV) and mRNA encapsulation efficiency (EE) of LNPs used in this work.

2.7. *In vivo delivery*

mRNA encoding Luciferase was administered into OF1 mice using LNPs via intravenous (retro orbital) injection. 24 h after injection, mice were anesthetized by CO_2. The organs of interest were dissected, rinsed in PBS (x 1) and mixed with an ULTRA-TURRAX™ homogenized in 1 mL for spleen and in 2 mL for lung and liver of lysis buffer x1 (Promega). Each organ mix was frozen at −80 °C, thawed and an aliquot of 0.5 mL was taken for luciferase analysis. The aliquot was centrifuged for 5 min at 12 000 rpm at 4 °C. Luciferase enzyme activity was assessed on 5 µL of organ lysate supernatant using 100 µL of luciferin solution (Promega). The luminescence (expressed as RLU) was measured by using a luminometer (Centro LB 960, Berthold) and normalized per mg of organ protein with Pierce BCA Assay Protein Kit (Thermo-Fisher).

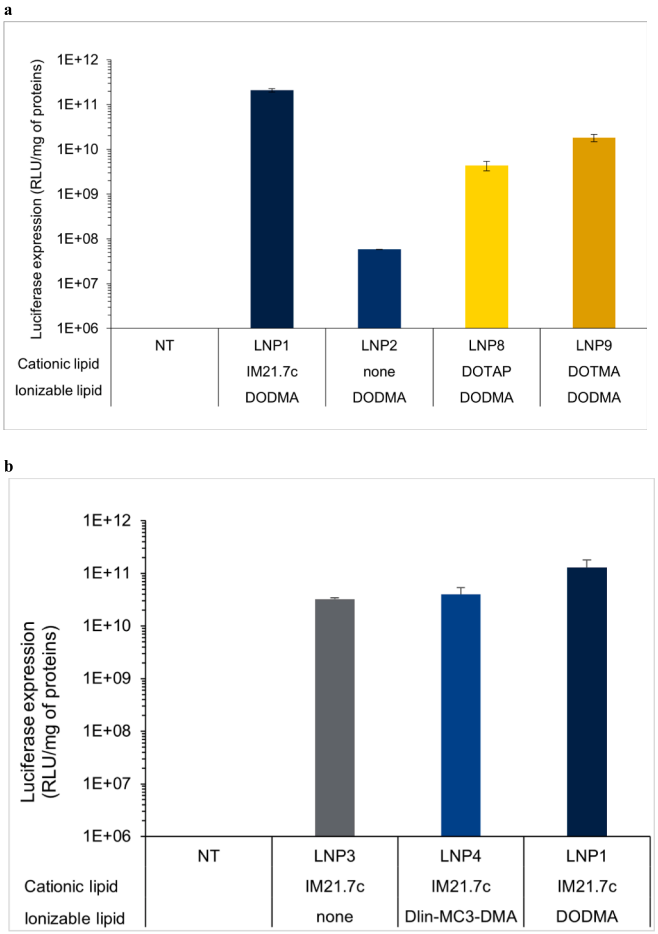

Fig. 2. Evaluation of imidazolium / DODMA requirement for LNP efficacy. (a, b and c) Caco-2 were transfected with LNPs (50 ng/µL of mRNA) using 500 ng of mRNA encoding Luciferase for 40,000 Caco-2 cells. Luciferase expression was assessed 24 h after transfection. (a) Evaluation of cationic lipid LNP1: IM21.7c/DODMA, LNP2: none/DODMA, LNP8: DOTAP/DODMA and LNP9: DOTMA/DODMA. NT: non-transfected cells. (b) Evaluating DODMA requirement for LNP efficacy: LNP3: IM21.7c/none, LNP4: IM21.7c/DLin-MC3-DMA and LNP1: IM21.7c/DODMA. (c) Optimization of imidazolium IM21.7c/ionizable lipid DODMA ratio: LNP5 2 mM/5 mM, LNP6 3 mM/3 mM, LNP7 4 mM/2 mM and LNP1 4 mM/3 mM (d) 7.5 µg of mRNA encoding Luciferase was injected into mice using LNPs (200 ng/µL mRNA) through intravenous injection (*retro*-orbital injection). LNP24: IM21.7c/DODMA, LNP27: IM21.7c/none and LNP28: DOTAP/DODMA. Luciferase expression was assessed 24 h post-injection. Mean ± SD were calculated and expressed relative to the protein level present in each organ (n = 3).

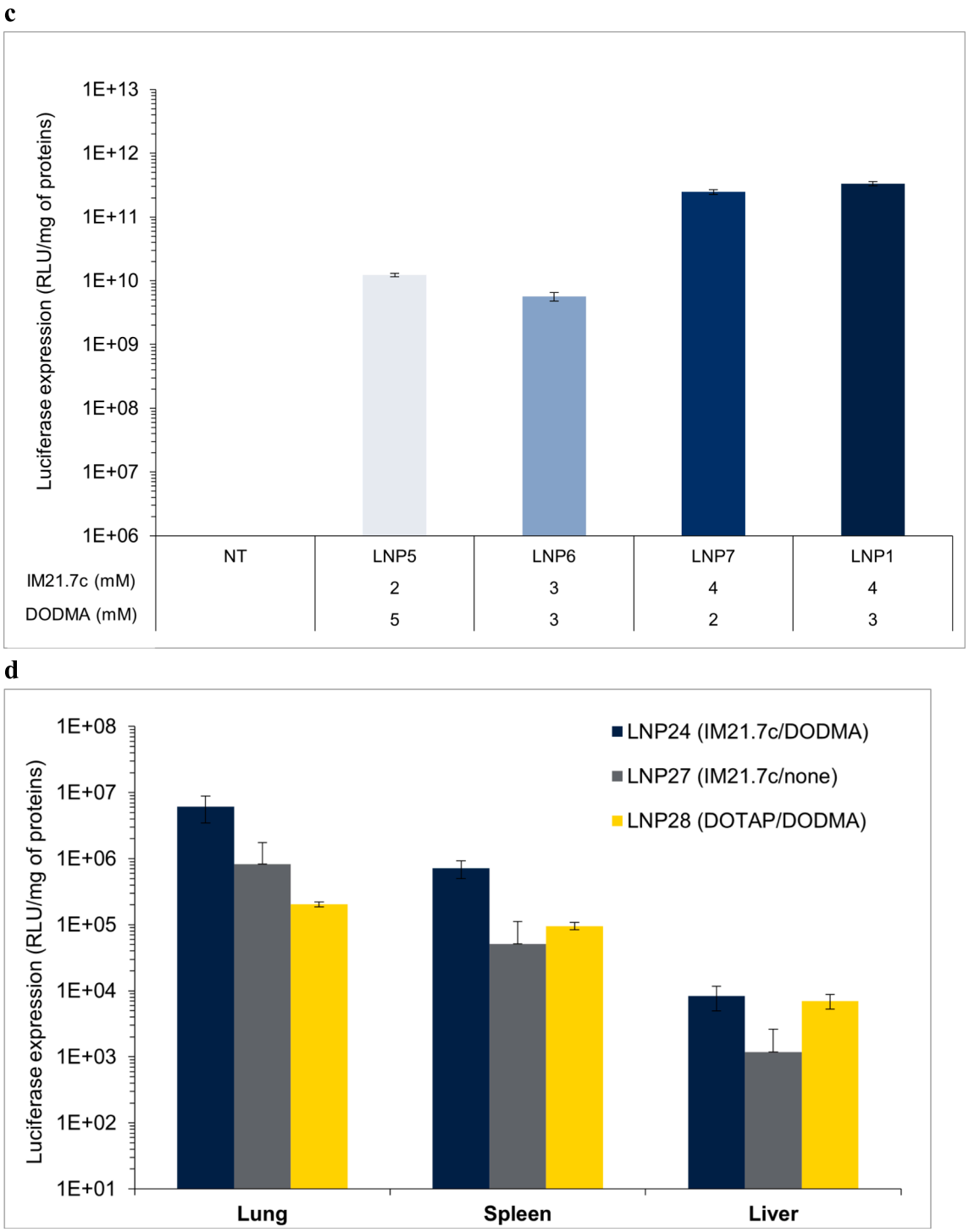

Fig. 2. (*continued*).

3. Results

3.1. Combinatorial approach to screening of mRNA-LNP formulations with imidazolium

3.1.1. Rationale

Recent developments have focused on reducing toxicity of cationic polymers and cationic lipids widely used for gene delivery and on expanding the biodistribution of ionisable lipids [8]. With this in mind, we have developed a new family of cationic molecules with an N-heterocycle (imidazolium) to be used for RNA delivery (patent number EP3646854). The design of this new family of molecules was based on 2 main principles: hide the permanent charge and induce a cone-shaped lipid [9]. Here we present a study aimed at developing imidazolium-based LNPs using the flagship IM21.7c capable of efficiently incorporating and delivering mRNA *in vitro* and *in vivo*, with a different biodistribution compared to currently clinically approved LNPs based on 4-lipid components including an ionizable lipids shown in Fig. 1.

*3.1.2. Comparison of LNPs with different cationic lipids (**IM21.7c**, DOTAP or DOTMA)*

To determine the most functional **IM21.7c** imidazolium-based

mRNA-LNPs systematically, we tested series of lipid formulations capable of encapsulating mRNA, using a range of lipid combinations and ratios. The LNPs were characterised in terms of size, zeta potential, polydispersity, encapsulation efficiency (Table 1 and Table S1) prior to being evaluated for *in vitro* transfection in Caco-2 cells and *in vivo* delivery (Figs. 2, 3 and 4). Formulations containing **IM21.7c** required a total of 5 lipid components: cationic lipid (**IM21.7c**), an ionizable lipid, a helper lipid, cholesterol and PEG-lipid derivatives. As expected, the use of a permanent cationic lipid **IM21.7c** is required to obtain positively charged LNPs at physiological pH (in Table 1, LNP1 is positively charged (+12 mV) compared to LNP2 which is neutral). We also compared the impact of **IM21.7c** against other well-known cationic lipids by varying only the nature of the cationic lipid in the formulation of the mRNA-LNPs (LNP1 containing **IM21.7c** versus LNP8 and LNP9

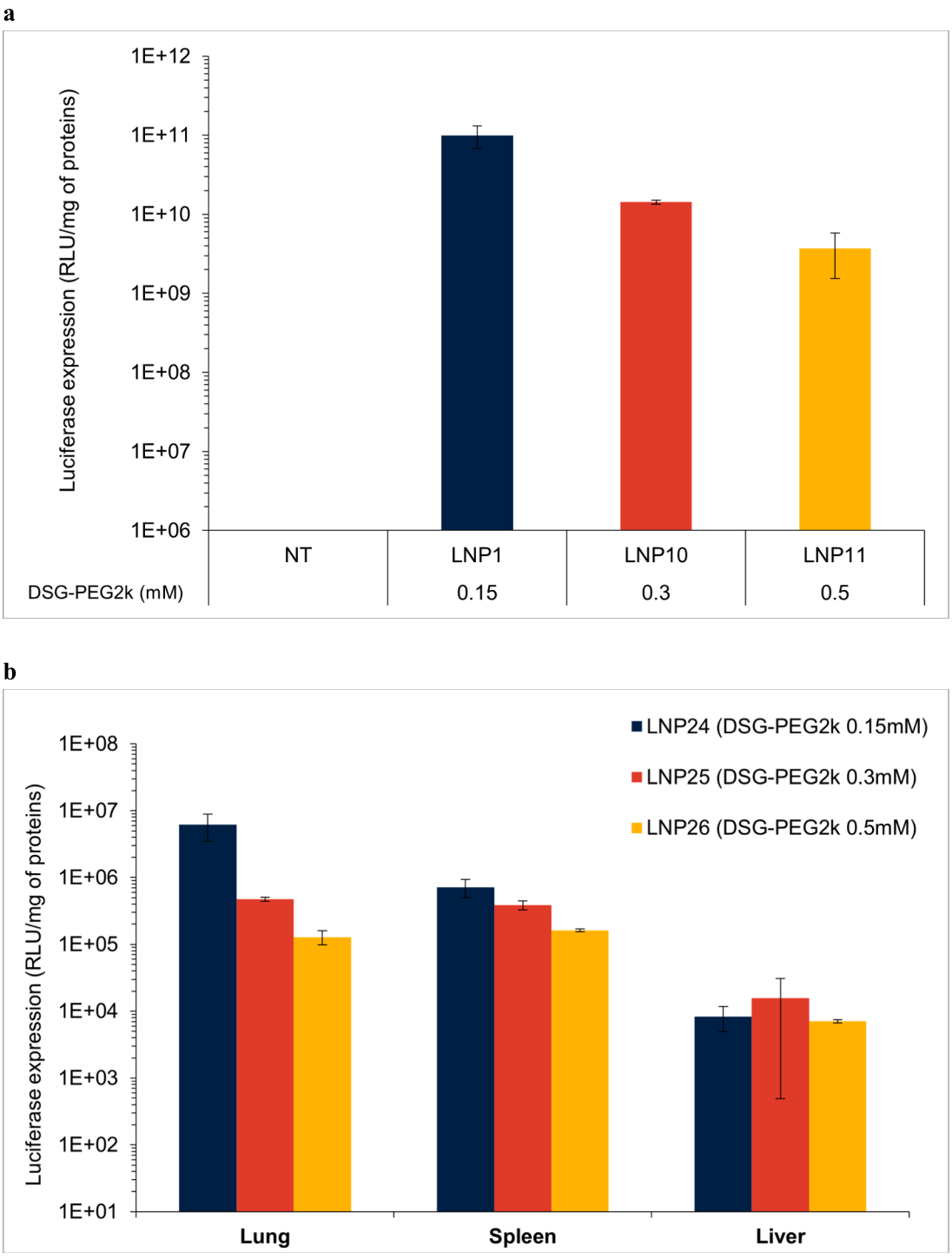

Fig. 3. Influence of the amount of PEG-Lipid *in vitro* and *in vivo*. (a) Caco-2 were transfected with LNPs (50 ng/μL of mRNA) using 500 ng of mRNA encoding Luciferase for 40,000 Caco-2 cells. Luciferase expression was assessed 24 h after transfection. LNP1: DSG-PEG 0.15 mM, LNP10: DSG-PEG 0.3 mM and LNP11: DSG-PEG 0.5 mM. NT: non-transfected cells. (b) 7.5 μg of mRNA encoding Luciferase was injected into mice using LNPs (200 ng/μL mRNA) through intravenous injection (*retro*-orbital injection). LNP24: DSG-PEG 0.15 mM, LNP25: DSG-PEG 0.3 mM and LNP26: DSG-PEG 0.5 mM. Luciferase expression was assessed 24 h post-injection. Mean ± SD were calculated and expressed relative to the protein level present in each organ (n = 3).

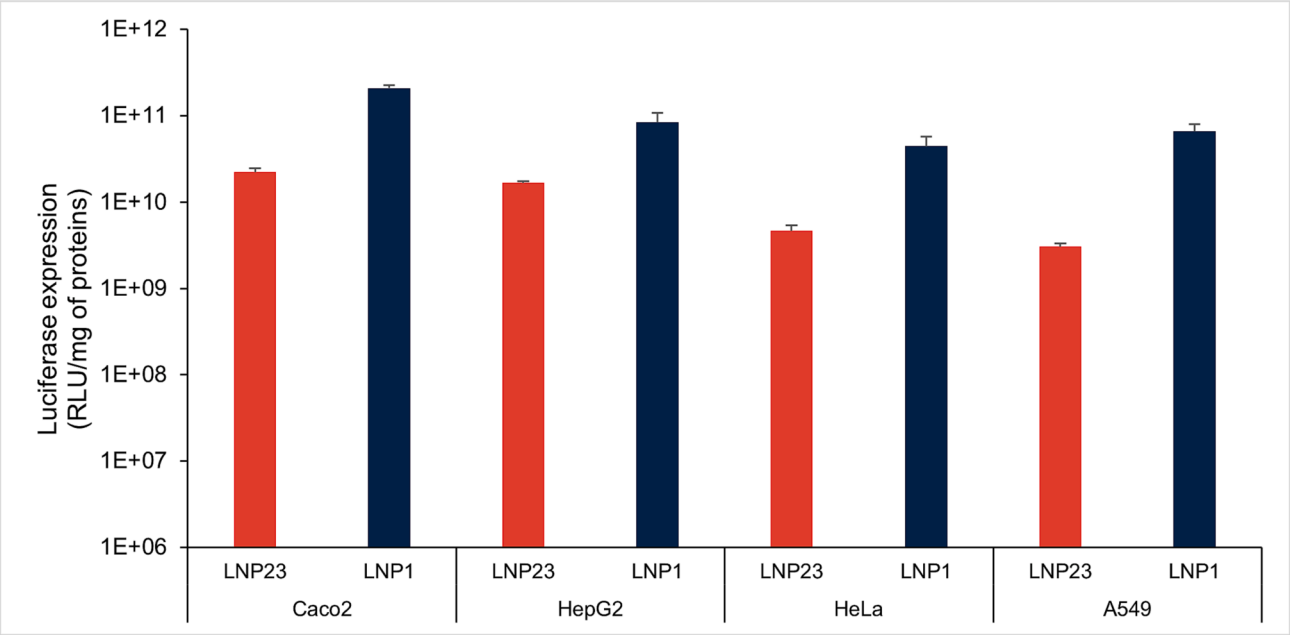

Fig. 4. ***In vitro*** **evaluation of LNPs with IM21.7c on different cell lines**. Caco-2 (40,000 cells), HepG2 (100,000 cells), HeLa (50,000 cells) and A549 (60,000 cells) cells were transfected with LNPs (50 ng/μL of mRNA) using 500 ng (Caco-2, HepG2 and A549) or 250 ng (HeLa) of Fluc-encoding mRNA. LNP23 (similar to Comirnaty® composition) was used as a positive transfection control (ALC-0315 4.63 mM/DSPC 0.94 mM/Cholesterol 4.27 mM/DMG-PEG_{2k} 0.16 mM). LNP1: IM21.7c 4 mM /DODMA 3 mM/DPyPe 1 mM/Cholesterol 1.85 mM/DSG-PEG_{2k} 0.15 mM. Luciferase expression was assessed 24 h after transfection.

containing DOTAP and DOTMA respectively). All three mRNA-LNPs (LNP1, LNP8 and LNP9) were small in size (less than 100 nm) and positively charged with a zeta potential between 10 and 20 mV (Table 1 and Table S1), however LNP1 formulated with N-heterocycle **IM21.7c** showed a transfection efficiency $> 10^{11}$ (RLU/mg of proteins), which was 10 times higher compared to LNPs with quaternary ammonium (LNP8 and LNP9 shown in Fig. 2a) or 10^3 higher than LNP without **IM21.7c** (LNP2).

3.1.3. Requirement for an ionizable lipid in addition to IM21.7c for mRNA-LNPs

We then tested the requirement for an ionizable lipid in the formulation. While **IM21.7c** based LNPs without an ionizable lipid (4-lipid formulation) formed nanoparticles suitable for *in vivo* administration of the size less than 100 nm and positively charged, with high encapsulation efficiently (>90%, Table 1, LNP3), this formulation however showed the lowest *in vitro* transfection efficiency compared to 5-lipid formulations (Fig. 2 b). We then also compared formulations with two common ionizable lipids, namely DODMA and DLin-MC3-DMA to select the most suitable one to be used in conjunction with IM21.7c; the incorporation of both noticeably improved mRNA-LNPs transfection efficiency compared to a 4-component formulation without an ionizable lipid; without modifying the LNP physical properties (Fig. 2a, LNP1 and LNP4). The LNPs with DODMA had a higher efficiency ($1.3x10^{11}$ RLU/mg of proteins) compared to those containing DLin-MC3-DMA ($4x10^{10}$ RLU/mg of proteins), making it the ionisable lipid of choice for further studies.

Having selected DODMA as the ionizable lipid of choice for the **IM21.7c** based mRNA-LNPs, we tested a range of different ratios of those two molecules (Table 1 and LNP12-18 in Table S1). An equimolar ratio of **IM21.7c** and DODMA (LNP6), or an excess of DODMA (LNP5) gave the lowest transfection efficiencies (Fig. 2c). The highest transfection efficiencies were achieved with 4 mM of **IM21.7c** and 2 or 3 mM of DODMA (LNP7 and LNP1, respectively). A concentration of 3 mM of DODMA was slightly more favourable and was selected for further evaluation *in vivo*.

Additionally, we also observed that the typical lipid composition of LNP formulation similar to Onpattro®, SpikeVax®, Comirnaty® [32] (LNP8 & LNP9 *in vitro*) loses its functionality when the ionizable lipid is replaced by IM21.7c. Additionally, the formulation using DSPC, phosphatidylcholine derivates or DOPE was not as efficient *in vitro* as DPyPE, a phospholipid with ramified alkyl chains (Fig. S3a).

3.1.4. In vivo evaluation of IM21.7c based LNPs

Next, we tested the mRNA-LNP delivery *in vivo* following intravenous (IV) delivery (Fig. 2d). LNPs contained 4 mM of cationic lipid (IM21.7c or DOTAP) and 3 mM of DODMA, as per the *in vitro* data (Fig. 2b) but higher mRNA concentration (200 ng/μl) to allow *in vivo* delivery. When LNPs contained **IM21.7c** as a cationic lipid (LNP24), luciferase expression was increased in the lung ($6.2x10^6$ versus $2.0x10^5$ RLU/mg of proteins) compared to the DOTAP-based LNPs (LNP28). There was also a slight increase in the spleen compared to DOTAP based LNPs (7.10^5 RLU/mg of proteins for LNP24 versus 1.10^5 RLU/mg of proteins for LNP28). The expression in the liver however was comparable (Fig. 2d). When IM21.7c was depleted of DODMA (LNP27), the luciferase expression decreased in all organs (lung, spleen and liver) (Fig. 2d), confirming that the combination of **IM21.7c** with DODMA is crucial to enhance *in vivo* mRNA delivery, similarly to the data obtained *in vitro* (Fig. 2a, c with LNP1 and 3. Taken together, these experiments show the potential of IM21.7c to improve targeting and gene expression of mRNA to the lung and spleen, when formulated with the ionizable lipid DODMA.

3.1.5. Role of helper lipids for functional IM21.7c mRNA-LNP formulations in vitro and in vivo

We next assessed the function and optimal concentration of PEG-lipid, as it is also critical for charge, stability and shielding effect. We formulated LNPs with 4 mM of **IM21.7c**, 3 mM of DODMA, 1 mM of DPyPE, 1.85 mM of cholesterol and an increasing concentration of DSG-PEG_{2k} or DMG-PEG_{2k}. Higher polydispersity (Table 1 and Table S1) and lower transfection efficiency (Fig. S1b) was observed with DMG-PEG_{2k} (LNP22 in Table S1) compared with DSG-PEG_{2k} (LNP1), ruling it out as a PEG-lipid for **IM21.7c** LNP formulations.

We then tested increasing concentrations of DSG-PEG (0.15, 0.3 and

0.5 mM) in the mRNA-LNPs. Interestingly, increasing the amount of DSG-PEG$_{2k}$ (LNP1, LNP10 and LNP11) lead to a reduction in particle size, with LNPs measuring 64 nm, 32 nm and 22 nm, respectively, without modifying the zeta potential (+12 to + 17 mV) or the mRNA encapsulation efficiency (Table 1 and Table S1). The LNPs with more DSG-PEG, namely LNP10 and LNP11 were less efficient in terms of transfection efficiency compared to LNP1 with 0.15 mM DSG-PEG in Caco-2 cells (Fig. 3a). The smaller LNPs containing 0.3 nM DSG-PEG (LNP31) of 41 nm were however more efficient at transfecting human primary T cells compared to the larger one (85 nm, LNP30) with 0.15 nM DSG-PEG (Fig. S1). Finally, as smaller LNPs are sometimes more effective at *in vivo* nucleic acid delivery, we tested *in vivo* mRNA delivery with LNPs composed of increasing concentration of DSG-PEG (Fig. 3b). The biodistribution of the 3 LNPs were comparable in the liver and spleen; however, the larger LNPs (97 nm) with the initial concentration of 0.15 mM DSG-PEG showed a significant increase of luciferase expression in the lung after IV delivery, confirming previous observations (Fig. 2d).

Taken together this analysis enabled the selection of the most promising formulations for *in vivo* nucleic acid delivery, showing that the formulation of choice for an imidazolium based LNP contains **IM21.7c** 4 mM, DODMA 3 mM, DPyPE 1 mM, Cholesterol 1.85 mM, DSG-PEG 0.15 mM.

3.2. Comparison of mRNA-LNP formulation based on IM21.7c imidazolium with clinically approved formulations based on ionizable lipids in vitro and in vivo

To evaluate these novel cationic LNPs, we compared them with another clinically approved ionizable lipid-based formulation, similar to Comirnaty® (BioNTech). We compared this 4-component nanoparticle containing an ionizable lipid (LNP23: ALC-0315 4.63 mM, DSPC 0.94 mM, Chol 4.27 mM and DMG-PEG 0.16 mM) to the most effective 5-component imidazolium-based (LNP1: **IM21.7c** 4 mM, DODMA 3 mM, DPyPE 1 mM, Cholesterol 1.85 mM, DSG-PEG 0.15 mM) for their transfection efficiency in cell lines derived from different tissues (Fig. 4). We tested transfection of colon carcinoma cells (Caco-2), hepatocarcinoma cells (HepG2), adenocarcinoma alveolar cells (A549) and cervical carcinoma cells (HeLa). In all cell lines, the IM21.7c imidazolium-based LNPs had a transfection efficiency at least 10-fold higher, ranging from 5.10^{10} to 2.10^{11} RLU/mg proteins) showing a significant improvement compared to the 4-component LNP formulations (Fig. 4).

To demonstrate that cationic lipid IM21.7c can be used in LNP formulation to transfect primary cells, LNP30 and LNP31 have been evaluated in Human primary T cells. Boths LNPs achieved high GFP expression (62% and 73% respectively, Fig. S2).

The biodistribution of **IM21.7c** based mRNA-LNP (5 components) was compared with another clinically approved 4-component formulation (Onpattro®, Alnylam) following IV delivery in mice (Fig. 5). (See Table S1 *in vivo* for characterisation of the LNPs and compare LNP24 with LNP29). Both formulations showed comparable expression in the spleen, however the DLin-MC3-DMA-based LNP showed a 100-fold higher *in vivo* mRNA delivery to the liver compared to the imidazolium-based one. In contrast, the **IM21.7c** imidazolium-LNP was much more efficient at achieving higher expression in the lung with $6x10^6$ versus $1x10^5$ RLU/mg of proteins measured by luciferase assay, emphasising a significant difference in biodistribution between the two formulations. We also evaluated intramuscular (IM) delivery of the IM21.7c-based LNP, which was as effective as a cationic liposome-based formulation used as a positive control (*in vivo*-jetRNA®+, Polyplus-transfection) (data not shown).

As some cationic lipids used in cationic liposomes or lipoplexes have been reported to induce some toxicity [29] (mainly liver toxicity and/or immune response), we checked the safety profile of **IM21.7c** based LNPs. First, we observed no mortality during our *in vivo* injections both IV and IM. We also quantified the pro-inflammatory response of the new **IM21.7c** based LNP following IV delivery. We determined a full cytokine profile including IFN-γ and TNF-α. Interestingly, the profile was much lower than the positive control (LPS) and comparable to the 4-lipid formulation with DLin-MC3-DMA as an ionizable lipid, except for IL-10 and IL-12 which were slightly increased at 24 h (Fig. S3). However, the secretion of some cytokines (IL-1α and IL-6, and to a lesser extent

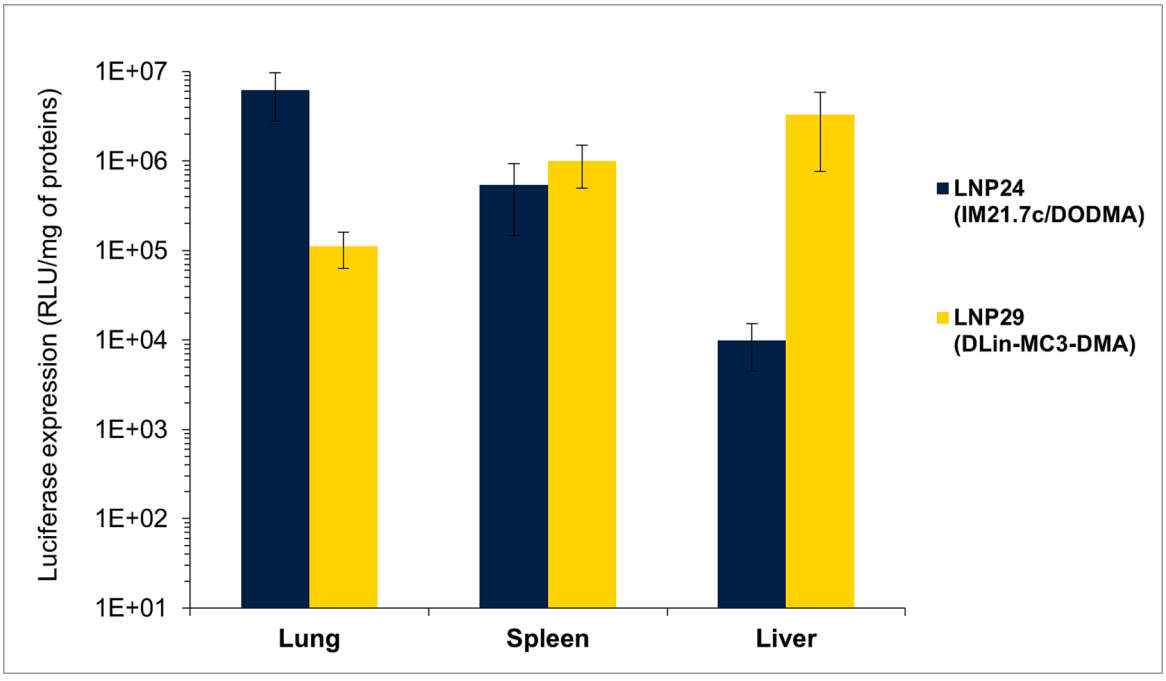

Fig. 5. LNPs with IM21.7c lead to a different biodistribution than LNP with ionizable lipids. 10 μg of mRNA encoding Luciferase was injected into mice using LNP24 or LNP29 (200 ng/μL mRNA) through intravenous injection (*retro*-orbital injection). LNP24: IM21.7c 4 mM /DODMA 3 mM/DPyPe 1 mM/Cholesterol 1.85 mM/DSG-PEG$_{2k}$ 0.15 mM and LNP29: Dlin-MC3-DMA 2.75 mM/DSPC 0.55 mM/Cholesterol 2.12 mM/DMG-PEG 0.08 mM. Luciferase expression was assessed 24 h post-injection. Mean ± SD were calculated and expressed relative to the protein level present in each organ (n = 6).

IL-1β and IL-10) following the injection of the 4- or 5-lipid formulations could be caused by the lipids or by the mRNA which is only modified with 5-methoxyuridine and not designed to reduce this pro-inflammatory response. Overall, this analysis shows that the IM21.7c-based LNP present a good safety profile in line with other clinically approved formulation and is thus suitable for further *in vivo* use in a clinical context.

3.3. Conclusion & discussion

The data presented shows a rational approach to the design of a new type of LNP suitable for mRNA delivery containing **IM21.7c** as a permanently charged cationic lipid. Given the structure of **IM21.7c**, an additional ionizable lipid was required for optimal transfection efficiency. This 5-lipid formulation is composed of materials which were principally chosen because of their contribution to LNP stability and genetic material incorporation. DODMA was selected due to its ionizable form that can further increase mRNA concentration in LNPs, and for its role in enhancing endosomal escape [13]. The phospholipid DPyPE was chosen to fulfil a structural role given its high stability as well as its ability to fuse with cell and endosomal membranes. Cholesterol was incorporated to further enhance LNP stability through improved membrane rigidity and integrity and as it is often associated with higher transfection efficiencies. This function is likely to be due to enhanced endosomal escape owing to its crystalline form on LNP surfaces that can promote membrane fusion. Lastly, the lipid-polymer conjugate DSG-PEG, well known for particle stability and nucleic acid encapsulation demonstrated a good compatibility with the use of **IM21.7c**. The particle size can be modulated by increasing the amount of DSG-PEG without affecting the particle charge. The resulting LNPs expand the 5-component LNP formulations [31] were compared to commercially available and clinically approved 4-lipid LNPs shown in Fig. 1.

Here we found that most effective **IM21.7c** based mRNA LNPs formulated for *in vivo* delivery (LNP24) are less than 100 nm diameter, slightly positively charged and encapsulating mRNA with an efficacy of 98 %. Due to a positive zeta potential induced by the permanently charged lipid IM21.7c, the biodistribution of these particles was different from other known ionizable and cationic lipids clinically approved which are typically mostly expressed in the liver [33]. The **IM21.7c** based LNPs induced high protein expression in the lung which was significantly higher (10-fold) than other known LNP formulations.

The physical properties of LNPs such as particle size, polydispersity, and surface charge are key characteristics to take into account when establishing a screening workflow to select effective *in vivo* delivery vehicles as they give insights into the structure and the stability of the LNPs. In this study, the positive particle charge seems to be a key indicator of *in vivo* fate as previously observed [34].

This preliminary study shows the potential of **IM21.7c** based LNPs for mRNA delivery, which is strengthened by the straightforward manufacturing process of these new LNPs, similar to those currently clinically approved (4-lipid compositions based on ionizable lipid). While findings from this study may open new avenues for the treatment of chronic and infectious lung diseases as well as for mRNA vaccination programs for infectious diseases and cancer immunotherapy [32], imidazolium-based mRNA LNPs remain to be evaluated for therapeutic efficacy.

Author contributions

C.G., M.H. and P.E. conceived the project. C.G. and M.H. designed the experiment. T.B.C., M.S., M.B., M.Z. and K.R. performed the main experiments. C.G. provided experimental support. C.G. and M.H. analyzed the data and wrote the manuscript. P.E. supervised the research and revised the manuscript.

CRediT authorship contribution statement

Claire Guéguen: Conceptualization, Methodology, Investigation, Formal analysis, Data curation, Writing – review & editing. **Thibaut Ben Chimol:** Investigation, Methodology, Resources. **Margaux Briand:** Investigation, Methodology, Resources. **Kassandra Renaud:** Investigation, Methodology, Resources. **Mélodie Seiler:** Investigation, Methodology, Resources. **Morgane Ziesel:** Investigation, Methodology, Resources. **Patrick Erbacher:** Conceptualization, Methodology, Writing – review & editing. **Malik Hellal:** Conceptualization, Methodology, Investigation, Formal analysis, Data curation, Writing – review & editing.

Declaration of Competing Interest

The authors declare that they have no known competing financial interests or personal relationships that could have appeared to influence the work reported in this paper.

Data availability

Data will be made available on request.

Acknowledgments

We thank Nathan CHABOCHE, Guillaume FREUND and Maria Nicla LOVIGLIO for critical reading of the manuscript.

Appendix A. Supplementary material

Supplementary data to this article can be found online at https://doi.org/10.1016/j.ejpb.2023.08.002.

References

[1] U. Sahin, A. Muik, E. Derhovanessian, I. Vogler, L.M. Kranz, M. Vormehr, A. Baum, K. Pascal, J. Quandt, D. Maurus, S. Brachtendorf, V. Lörks, J. Sikorski, R. Hilker, D. Becker, A.-K. Eller, J. Grützner, C. Boesler, C. Rosenbaum, M.-C. Kühnle, U. Luxemburger, A. Kemmer-Brück, D. Langer, M. Bexon, S. Bolte, K. Karikó, T. Palanche, B. Fischer, A. Schultz, P.-Y. Shi, C. Fontes-Garfias, J.L. Perez, K. A. Swanson, J. Loschko, I.L. Scully, M. Cutler, W. Kalina, C.A. Kyratsous, D. Cooper, P.R. Dormitzer, K.U. Jansen, Ö. Türeci, COVID-19 vaccine BNT162b1 elicits human antibody and TH1 T cell responses, Nature 586 (7830) (2020) 594–599.

[2] K. Wu, A.P. Werner, M. Koch, A. Choi, E. Narayanan, G.B.E. Stewart-Jones, T. Colpitts, H. Bennett, S. Boyoglu-Barnum, W. Shi, J.I. Moliva, N.J. Sullivan, B. S. Graham, A. Carfi, K.S. Corbett, R.A. Seder, D.K. Edwards, Serum Neutralizing Activity Elicited by mRNA-1273 Vaccine, N. Engl. J. Med. 384 (15) (2021) 1468–1470.

[3] L.R. Baden, H.M. El Sahly, B. Essink, K. Kotloff, S. Frey, R. Novak, D. Diemert, S. A. Spector, N. Rouphael, C.B. Creech, J. McGettigan, S. Khetan, N. Segall, J. Solis, A. Brosz, C. Fierro, H. Schwartz, K. Neuzil, L. Corey, P. Gilbert, H. Janes, D. Follmann, M. Marovich, J. Mascola, L. Polakowski, J. Ledgerwood, B.S. Graham, H. Bennett, R. Pajon, C. Knightly, B. Leav, W. Deng, H. Zhou, S. Han, M. Ivarsson, J. Miller, T. Zaks, Efficacy and Safety of the mRNA-1273 SARS-CoV-2 Vaccine, N. Engl. J. Med. 384 (5) (2021) 403–416.

[4] M.D. Buschmann, M.J. Carrasco, S. Alishetty, M. Paige, M.G. Alameh, D. Weissman, Nanomaterial Delivery Systems for mRNA Vaccines, Vaccines 9 (1) (2021) 65.

[5] A.K. Blakney, P.F. McKay, C.R. Bouton, K. Hu, K. Samnuan, R.J. Shattock, Innate Inhibiting Proteins Enhance Expression and Immunogenicity of Self-Amplifying RNA, Mol. Ther. 29 (3) (2021) 1174–1185.

[6] A.J. Geall, A. Verma, G.R. Otten, C.A. Shaw, A. Hekele, K. Banerjee, Y. Cu, C. W. Beard, L.A. Brito, T. Krucker, D.T. O'Hagan, M. Singh, P.W. Mason, N. M. Valiante, P.R. Dormitzer, S.W. Barnett, R. Rappuoli, J.B. Ulmer, C.W. Mandl, Nonviral delivery of self-amplifying RNA vaccines, Proc. Natl. Acad. Sci. 109 (36) (2012) 14604–14609.

[7] A.K. Blakney, P.F. McKay, B.I. Yus, Y. Aldon, R.J. Shattock, Inside out: optimization of lipid nanoparticle formulations for exterior complexation and in vivo delivery of saRNA, Gene Ther. 26 (9) (2019) 363–372.

[8] M.J. Mitchell, M.M. Billingsley, R.M. Haley, M.E. Wechsler, N.A. Peppas, R. Langer, Engineering precision nanoparticles for drug delivery, Nat. Rev. Drug Discov. 20 (2) (2021) 101–124.

[9] J.A. Kulkarni, P.R. Cullis, R. van der Meel, Lipid Nanoparticles Enabling Gene Therapies: From Concepts to Clinical Utility, Nucleic Acid Ther. 28 (3) (2018) 146–157, https://doi.org/10.1089/nat.2018.0721.

[10] C. Hald Albertsen, J.A. Kulkarni, D. Witzigmann, M. Lind, K. Petersson, J. B. Simonsen, The role of lipid components in lipid nanoparticles for vaccines and gene therapy, Adv. Drug Deliv. Rev. 188 (2022) 114416.

[11] Y. Zhang, C. Sun, C. Wang, K.E. Jankovic, Y. Dong, Lipids and Lipid Derivatives for RNA Delivery, Chem. Rev. 121 (20) (2021) 12181–12277.
[12] D. Simberg, S. Weisman, Y. Talmon, Y. Barenholz, DOTAP (and other cationic lipids): chemistry, biophysics, and transfection, Crit. Rev. Ther. Drug Carrier Syst. 21 (4) (2004) 257–317.
[13] M. Maugeri, M. Nawaz, A. Papadimitriou, A. Angerfors, A. Camponeschi, M. Na, M. Hölttä, P. Skantze, S. Johansson, M. Sundqvist, J. Lindquist, T. Kjellman, I.-L. Mårtensson, T. Jin, P. Sunnerhagen, S. Östman, L. Lindfors, H. Valadi, Linkage between endosomal escape of LNP-mRNA and loading into EVs for transport to other cells, Nat. Commun. 10 (1) (2019), https://doi.org/10.1038/s41467-019-12275-6.
[14] S.T. LoPresti, M.L. Arral, N. Chaudhary, K.A. Whitehead, The replacement of helper lipids with charged alternatives in lipid nanoparticles facilitates targeted mRNA delivery to the spleen and lungs, J. Control. Release 345 (2022) 819–831.
[15] M. Yanez Arteta, T. Kjellman, S. Bartesaghi, S. Wallin, X. Wu, A.J. Kvist, A. Dabkowska, N. Székely, A. Radulescu, J. Bergenholtz, L. Lindfors, Successful reprogramming of cellular protein production through mRNA delivered by functionalized lipid nanoparticles, Proc. Natl. Acad. Sci. 115 (15) (2018), https://doi.org/10.1073/pnas.1720542115.
[16] R. Pattipeiluhu, G. Arias-Alpizar, G. Basha, K.Y.T. Chan, J. Bussmann, T.H. Sharp, M.-A. Moradi, N. Sommerdijk, E.N. Harris, P.R. Cullis, A. Kros, D. Witzigmann, F. Campbell, Anionic Lipid Nanoparticles Preferentially Deliver mRNA to the Hepatic Reticuloendothelial System, Adv. Mater. 34 (16) (2022) 2201095.
[17] M.L. Brader, S.J. Williams, J.M. Banks, W.H. Hui, Z.H. Zhou, L. Jin, Encapsulation state of messenger RNA inside lipid nanoparticles, Biophys. J . 120 (14) (2021) 2766–2770.
[18] Y. Xu, T. Fourniols, Y. Labrak, V. Préat, A. Beloqui, A. des Rieux, Surface Modification of Lipid-Based Nanoparticles, ACS Nano 16 (5) (2022) 7168–7196.
[19] M. Ripoll, M.-C. Bernard, C. Vaure, E. Bazin, S. Commandeur, V. Perkov, K. Lemdani, M.-C. Nicolaï, P. Bonifassi, A. Kichler, B. Frisch, J. Haensler, An imidazole modified lipid confers enhanced mRNA-LNP stability and strong immunization properties in mice and non-human primates, Biomaterials 286 (2022) 121570.
[20] S. Alishetty, et al., Novel lipid nanoparticle provides potent SARS-CoV-2 mRNA vaccine at low dose with low local reactogenicity, high thermostability and limited systemic biodistribution, Research Square, 2021.
[21] X. Han, H. Zhang, K. Butowska, K.L. Swingle, M.-G. Alameh, D. Weissman, M. J. Mitchell, An ionizable lipid toolbox for RNA delivery, Nat. Commun. 12 (1) (2021), https://doi.org/10.1038/s41467-021-27493-0.
[22] M. Cornebise, E. Narayanan, Y. Xia, E. Acosta, L. Ci, H. Koch, J. Milton, S. Sabnis, T. Salerno, K.E. Benenato, Discovery of a Novel Amino Lipid That Improves Lipid Nanoparticle Performance through Specific Interactions with mRNA, Adv. Funct. Mater. 32 (8) (2022) 2106727.
[23] M. Schlich, R. Palomba, G. Costabile, S. Mizrahy, M. Pannuzzo, D. Peer, P. Decuzzi, Cytosolic delivery of nucleic acids: The case of ionizable lipid nanoparticles, Bioeng. Transl. Med. 6 (2) (2021) e10213.
[24] M.J. Carrasco, S. Alishetty, M.-G. Alameh, H. Said, L. Wright, M. Paige, O. Soliman, D. Weissman, T.E. Cleveland, A. Grishaev, M.D. Buschmann, Ionization and structural properties of mRNA lipid nanoparticles influence expression in intramuscular and intravascular administration, Communications Biology 4 (1) (2021), https://doi.org/10.1038/s42003-021-02441-2.
[25] Leung, A.K.K. et al., Microfluidics Mixing: A general method for encapsulating macromolecules in lipid nanoparticle systems. *J. Phys. Chem. B* 2015, **119**, 28, 8698–8706. (https://doi.org/10.1021/acs.jpcb.5b02891).
[26] Sheperd S.J. Scalable mRNA and siRNA Lipid Nanoparticle Production Using a Parallelized Microfluidic Device. *Nano Lett.* 2021, **21**, 13, 5671. (https://doi.org/10.1021/acs.nanolett.1c01353).
[27] Sheperd S.J. et al. Microfluidic formulation of nanoparticles for biomedical applications. Biomaterials 2021, 274, 120826. (https://doi.org/10.1016/j.biomaterials.2021.120826).
[28] M. Maeki, et al., Microfluidic technologies and devices for lipid nanoparticle-based RNA delivery, Journal of Controlled Release 344 (2022) 80, https://doi.org/10.1016/j.jconrel.2022.02.017.
[29] H. Lv, S. Zhang, B. Wang, S. Cui, J. Yan, Toxicity of cationic lipids and cationic polymers in gene delivery, J. Control. Release 114 (1) (2006) 100–109.
[30] M.P. Lokugamage, D. Vanover, J. Beyersdorf, M.Z.C. Hatit, L. Rotolo, E. S. Echeverri, H.E. Peck, H. Ni, J.-K. Yoon, YongTae Kim, P.J. Santangelo, J. E. Dahlman, Optimization of lipid nanoparticles for the delivery of nebulized therapeutic mRNA to the lungs, Nat. Biomed. Eng. 5 (9) (2021) 1059–1068.
[31] M. Massaro, S. Wu, G. Baudo, H. Liu, S. Collum, H. Lee, C. Stigliano, V. Segura-Ibarra, H. Karmouty-Quintana, E. Blanco, Lipid nanoparticle-mediated mRNA delivery in lung fibrosis, Eur. J. Pharm. Sci. 183 (2023) 106370.
[32] L. Schoenmaker, D. Witzigmann, J.A. Kulkarni, R. Verbeke, G. Kersten, W. Jiskoot, D.J.A. Crommelin, mRNA-lipid nanoparticle COVID-19 vaccines: Structure and stability, Int. J. Pharm. 601 (2021) 120586.
[33] E. Blanco, H. Shen, M. Ferrari, Principles of nanoparticle design for overcoming biological barriers to drug delivery, Nat. Biotechnol. 33 (9) (2015) 941–951, https://doi.org/10.1038/nbt.3330.
[34] L. Miao, Y. Zhang, L. Huang, mRNA vaccine for cancer immunotherapy, Mol. Cancer 20 (1) (2021) 41, https://doi.org/10.1186/s12943-021-01335-5.